BAMS In Box

Is Weather Chaotic?

Coexistence of Chaos and Order within a Generalized Lorenz Model

Bo-Wen Shen, Roger A. Pielke Sr., Xubin Zeng, Jong-Jin Baik,
Sara Faghih-Naini, Jialin Cui, and Robert Atlas

ABSTRACT: Over 50 years since Lorenz's 1963 study and a follow-up presentation in 1972, the statement "weather is chaotic" has been well accepted. Such a view turns our attention from regularity associated with Laplace's view of determinism to irregularity associated with chaos. In contrast to single-type chaotic solutions, recent studies using a generalized Lorenz model (GLM) have focused on the coexistence of chaotic and regular solutions that appear within the same model using the same modeling configurations but different initial conditions. The results, with attractor coexistence, suggest that the entirety of weather possesses a dual nature of chaos and order with distinct predictability. In this study, based on the GLM, we illustrate the following two mechanisms that may enable or modulate two kinds of attractor coexistence and, thus, contribute to distinct predictability: 1) the aggregated negative feedback of small-scale convective processes that can produce stable nontrivial equilibrium points and, thus, enable the appearance of stable steady-state solutions and their coexistence with chaotic or nonlinear oscillatory solutions, referred to as the first and second kinds of attractor coexistence; and 2) the modulation of large-scale time-varying forcing (heating) that can determine (or modulate) the alternative appearance of two kinds of attractor coexistence. Based on our results, we then discuss new opportunities and challenges in predictability research with the aim of improving predictions at extended-range time scales, as well as subseasonal to seasonal time scales.

https://doi.org/10.1175/BAMS-D-19-0165.1
Corresponding author: Bo-Wen Shen, bshen@sdsu.edu
Supplemental material: https://doi.org/10.1175/BAMS-D-19-0165.2
In final form 16 September 2020

AFFILIATIONS: Shen—Department of Mathematics and Statistics, San Diego State University, San Diego, California; **Pielke**—Cooperative Institute for Research in Environmental Sciences, University of Colorado Boulder, Boulder, Colorado; **Zeng**—Department of Hydrology and Atmospheric Science, The University of Arizona, Tucson, Arizona; **Baik**—School of Earth and Environmental Sciences, Seoul National University, Seoul, South Korea; **Faghih-Naini**—Department of Mathematics and Statistics, San Diego State University, San Diego, California, and University of Bayreuth, Bayreuth, and Friedrich-Alexander University Erlangen–Nuremberg, Erlangen, Germany; **Cui**—Department of Mathematics and Statistics, and Department of Computer Sciences, San Diego State University, San Diego, California; **Atlas***—National Oceanic and Atmospheric Administration/AOML, Miami, Florida
*Retired

Our current view of "weather is chaotic" is based on the pioneering modeling study of Prof. Lorenz (Lorenz 1963a), who presented the sensitive dependence of solutions on initial conditions (SDIC), also known as the butterfly effect (Lorenz 1993). The feature of SDIC suggests that an initial tiny perturbation will eventually lead to a different time evolution of the solution. The conventional view has had a profound impact in meteorology for decades, in particular in numerical weather and climate predictions. However, recent findings obtained by analyzing and comparing the original Lorenz models (Lorenz 1963a, 1969, 1972) and the generalized Lorenz model (GLM; Shen 2019a,b; Shen et al. 2019) challenge the validity of the statement "weather is chaotic" in representing the true nature of weather. In this study, we provide new insights and opportunities using the GLM in order to formalize a revised view that focuses on the dual nature of chaos and order in weather, an "intuitive idea" that many meteorologists may unconsciously have, and to present approaches for improving our understanding of predictability and weather prediction at extended-range and subseasonal to seasonal time scales (e.g., Shen et al. 2010; Shen 2019b).

To achieve our goal, we first review three types of solutions within the Lorenz 1963 model and two kinds of attractor coexistence within the GLM, including coexisting chaotic and regular solutions. We then replace a time-independent parameter by a time-dependent model parameter in order to present the alternative and concurrent appearance of various types of solutions, showing the complexities in weather and climate. To facilitate discussions, two kinds of predictability are defined as follows: 1) intrinsic predictability that is only dependent on flow itself and 2) practical predictability that is limited by imperfect initial conditions and/or (mathematical) formulas (Lorenz 1963b; Shen 2014). Table 1 lists the definitions of concepts related to predictability.

Analysis and discussion

The Lorenz 1963 model and three types of solutions. The model used in the Lorenz 1963 study was derived from the governing equations of Rayleigh–Bénard convection with heating imposed on the bottom, and consists of three first-order ordinary differential equations (ODEs) for the three state variables that represent amplitudes for the Fourier modes of streamfunction and temperature. The state variables X, Y, and Z are referred to as primary scale modes to be distinguished from smaller-scale state variables that only appear within the GLM. To analyze a system of ODEs, state variables are often used as coordinates in order to construct the so-called phase space. The time evolution of a solution within the phase space is called an orbit or a trajectory. As a result of the three variables used as coordinates, the model is referred to as the three-dimensional Lorenz model (3DLM). In addition to the state variables, the 3DLM contains three, time-independent parameters that represent the strength of heating and dissipation, and the scale ratio of the convective cell. The strength of heating is determined by the normalized Rayleigh parameter (also called a heating parameter, denoted as r) that

Table 1. Definitions of concepts related to predictability in this study.

Name	Definitions	References
First kind of attractor coexistence	Coexistence of chaotic and steady-state solutions	Yorke and Yorke (1979), Shen (2019a)
Second kind of attractor coexistence	Coexistence of nonlinear oscillatory and steady-state solutions	Shen (2019a)
Attractor	The smallest attracting point set that, itself, cannot be decomposed into two or more subsets with distinct basins of attraction	Sprott et al. (2013)
Autonomous	A system of ODEs is autonomous if time does not appear explicitly within the equations	Jordan and Smith (2007)
Basin of attraction	As time advances, orbits initialized within a basin tend asymptotically to the attractor lying within the basin	Thompson and Stewart (2002)
Chaos	Orbits exhibit sensitive dependence on ICs	Lorenz (1993)
Computational chaos	Appearing "when the exact solution varies periodically with time, there is sometimes a range of time increment where the computed solution is chaotic"	Lorenz (2006)
Final state sensitivity	Nearby orbits settle to one of multiple attractors for a finite but arbitrarily long time	Grebogi et al. (1983)
Intransitivity	A specific type of solution lasts forever	Lorenz (1990)
Intrinsic predictability	Predictability that is only dependent on the flow itself	Lorenz (1963b) Shen (2014)
Limit cycle	Nonlinear oscillatory solution; an isolated closed orbit	Jordan and Smith (2007)
Nonautonomous	Variable time (τ) appears on the right-hand side of the equations	Jordan and Smith (2007)
Phase space	Within a system of the first-order ODEs, a phase space or state space can be constructed using time-dependent variables as coordinates	Hilborn (2000)
Practical predictability	Predictability that is limited by imperfect initial conditions and/or (mathematical) formulas	Lorenz (1963b) Shen (2014)
Recurrence	Defined when a trajectory returns back to the neighborhood of a previously visited state; recurrence may be viewed as a generalization of "periodicity" that includes quasi periodicity with multiple frequencies and chaos	Thompson and Stewart (2002)
Riddled basins	Basins with fractal boundaries in which every point in one basin of attraction is arbitrarily close to a point in the other basin	Alexander et al. (1992)
Sensitive dependence	The property characterizing an orbit if most other orbits that pass close to it at some point do not remain close to it as time advances	Lorenz (1993)

represents temperature differences between the top and bottom. Without a loss of generality, below, we discuss features of the 3DLM and GLM by only varying the heating parameter and keeping the remaining two parameters constant. The dependence of solutions on the other parameters can be found in Sparrow (1982).

As discussed in section 3.1 of Shen (2019b), each of the three types of solutions, including steady-state, chaotic, and nonlinear oscillatory solutions, may exclusively appear at small, medium, and large heating parameters, respectively (e.g., Sparrow 1982). The three types of solutions are also referred to as point, chaotic, and periodic attractors, respectively, and the latter is also known as a limit cycle solution (Shimizu 1979).[1] Intrinsic predictability for chaotic solutions is limited but unlimited for nonchaotic orbits. Within chaotic solutions, the degree of finite predictability varies, displaying a dependence on initial conditions (Slingo and Palmer 2011; Nese 1989; Zeng et al. 1993).

Missing features in the conventional view of "weather is chaotic."

By only applying chaotic solutions in order to define the nature of weather, an implicit assumption is that heating parameters

[1] Studies by Pedlosky (1972) and Smith and Reilly (1977) found that a limit cycle solution can be applied in order to understand amplitude vacillation, whose amplitude grows and periodically decays in a regular cycle (Lorenz 1963c; Ghil et al. 2010). Oscillatory solutions can be found in simplified or high-order, Lorenz-type models (e.g., Park et al. 2016; Moon et al. 2017, 2019, 2020; Faghih-Naini and Shen 2018; Shen 2018, 2019a, 2020, 2021).

must always stay within the specific interval of positive values. A consequence is that an initial tiny perturbation will always lead to a significant change in the time evolution of solutions (i.e., SDIC). However, neither the assumption nor the consequence has been verified against observations. Below, we first illustrate the impact of time-varying heating parameters on the appearance of chaotic solutions and then discuss the insensitivity of nonchaotic solutions to initial conditions.

Modulation of solutions by a time-varying heating function. Table 2 lists a periodic heating function with a time period of $2\pi T$ and two coefficients[2] (e.g., Franz and Zhang 1995), and the initial conditions for experiments using the 3DLM and GLM. The integration interval of dimensionless time τ is between 0 and $5\pi T$ (i.e., $\tau \in [0, 5\pi T]$). For the selected periodic heating function, $r \in [10, 350]$, we compare a control run to two parallel runs that add initial tiny perturbations of $\varepsilon = 10^{-8}$ and $\varepsilon = -10^{-8}$, respectively. As shown in Figs. 1a and 1b, the alternative appearance of three types of solutions is modulated by periodic heating. Zoomed-in views in Figs. 1c–e show 1) a SDIC as indicated by the divergences of initial nearby trajectories for a heating parameter larger than 24.74 (e.g., $\tau \in [28, 30]$), 2) chaotic solutions for $\tau \in [30.5, 32.5]$, and 3) regular oscillatory solutions at large heating parameters for $\tau \in [40, 42]$. These possess oscillatory features of limit cycle solutions that are defined using a constant heating parameter. As defined in Table 1, oscillatory features associated with a time-varying parameter may be referred to as recurrence. 4) Figure 1a additionally displays a transition from a stable steady-state solution, to an unstable steady-state solution, and then to a chaotic solution for $\tau \in [23, 30]$ (or $\tau \in [55, 62]$). Such a transition indicates an effective, but not necessarily realistic, growth of disturbance as a result of the nonexistence of stable equilibrium points for $r > 24.74$ (Lorenz 1963a). After being chaotic, associated with time-varying heating, all three trajectories become regularly oscillatory again, as shown in Fig. 1f for $\tau \in [72, 74]$. 5) *The appearance of a chaotic epoch with SDIC is modulated by periodic heating (i.e., the forcing)* and *SDIC may not be well-defined within the epoch of nonlinear oscillatory solutions, during which the differences of two initial nearby trajectories regularly vary.*

[2] As defined in Table 1, the system becomes nonautonomous (e.g., Lucarini 2019) since a time-varying parameter is considered. However, mathematically, such a system can be converted into an autonomous system as follows: we introduce a new state variable, p, in order to replace τ/T, yielding $r(\tau) = r_0 + r_1\sin(p)$ and $dp/d\tau = 1/T$. Then, the new system that consists of the 3DLM and an additional ODE for the new state variable p is autonomous. In this study, a change in (r_0, r_1, T) does not change our conclusion.

As documented in existing studies, initial small errors do not have a long-term impact on nonchaotic solutions, such as steady-state and oscillatory solutions (except for phases), consistent with our daily experiences. However, the exclusive appearance of single attractors suggests that initial tiny errors either have no impact or a large impact. Below, to provide a more realistic description of weather, we present a model that possesses the coexistence of chaotic and nonchaotic solutions.

Table 2. Model settings for numerical experiments within the 3DLM and GLM. The time-varying heating function is written as $r(\tau) = r_o + r_1 \sin(\tau/T)$. Here, τ represents nondimensional time and T is the time period of the heating function. The values of r_o and r_1 are selected in order to determine the specific range of values for the heating parameter.

	3DLM	GLM with 9 modes
Coefficients and period for the heating function	(r_o, r_1, T) = (180, 170,5)	(r_o, r_1, T) = (1,200, 520,5)
Initial conditions	(X, Y, Z) = (0, 1 + ε, 0)	(X, Y, Z) = (0, 1 + ε, 0)
	ε = 0, 10^{-8}, or -10^{-8}	The rest of state variables are set to 0
		ε = 0, 10^{-8}, or -10^{-8}

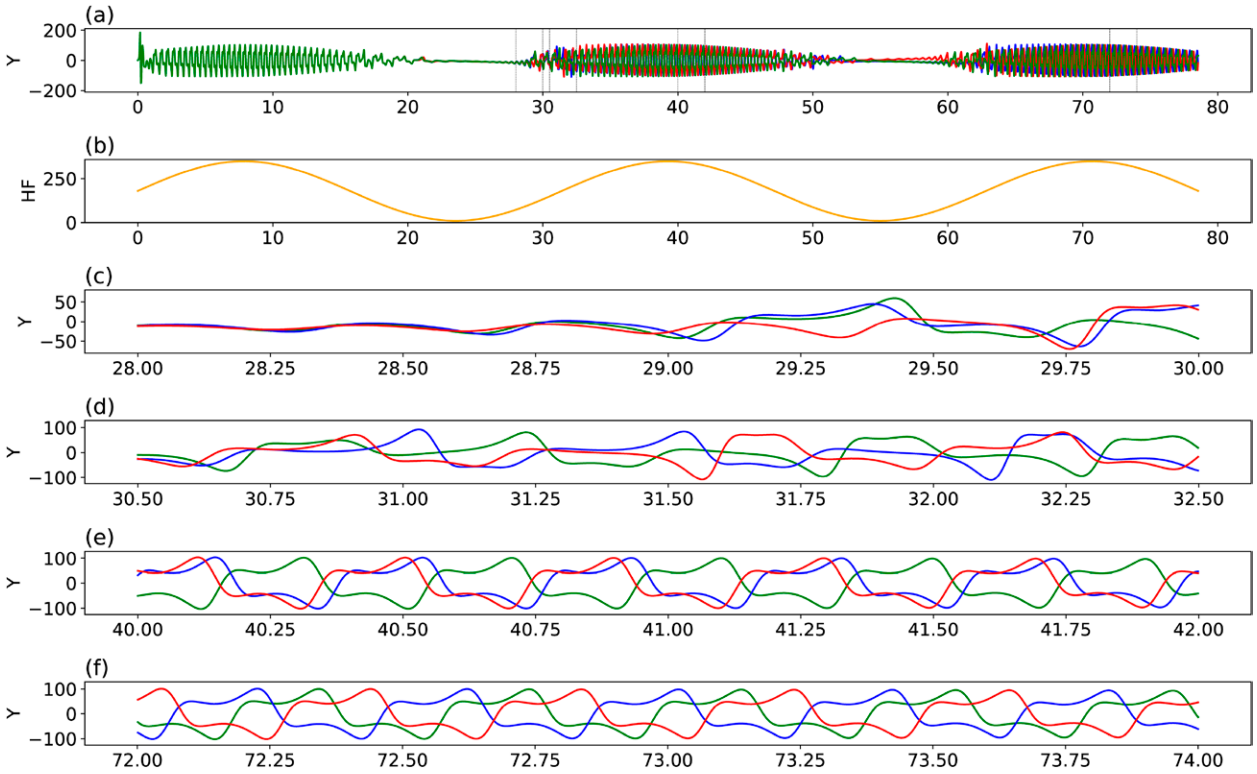

Fig. 1. The alternative appearance of three types of solutions modulated by the periodic heating function, $r = r_0 + r_1 \sin(\tau/T)$, within the 3DLM. The green line represents the solution of the control run, while blue and red lines display solutions obtained from parallel runs that include an initial tiny perturbation, $\varepsilon = 10^{-8}$ and $\varepsilon = -10^{-8}$, respectively. An orange line shows the heating function. (a),(b) The three orbits and the heating parameters for $\tau \in [0,5\pi T]$. (a) A pair of dashed vertical lines indicates the time interval used in (c)–(e). (c) $\tau \in [28, 30]$ reveals a transition to diverged trajectories, displaying sensitive dependence on initial conditions. After a transition from stable to unstable steady-state solutions, chaotic solutions appear, as shown in (d) for $\tau \in [30.5, 32.5]$. (e) $\tau \in [40, 42]$ displays nonlinear oscillatory solutions that are comparable to limit cycle solutions typically defined at large, time-independent heating parameters. After being chaotic and steady associated with time-varying heating, all three trajectories become regularly oscillatory again [e.g., for $\tau \in [72, 74]$ in (f)].

The generalized Lorenz model and two kinds of attractor coexistence. Attractor coexistence within conservative Hamiltonian systems has been documented for several decades (Hilborn 2000). Within dissipative systems, the coexistence of chaotic and nonchaotic solutions has also been discussed in some fields for more than two decades (e.g., Sprott et al. 2005). However, in meteorology,[3] related research activities using high-order, Lorenz-type systems still remain active. Below, we apply the GLM in order to discuss how coexisting attractors may better reveal the nature of weather.[4]

The GLM that allows any odd number of Fourier modes was derived based on the physical improvement of nonlinear temperature advection that is associated with mathematical extension of the nonlinear feedback loop within the 3DLM. A brief description of the GLM is provided in the online supplemental material (https://doi.org/10.1175/BAMS-D-19-0165.2). As shown in Fig. 1 of Shen (2019a), a comparison of the

[3] The 3DLM also possesses attractor coexistence (Yorke and Yorke 1979; Shen et al. 2021). However, such a feature has been overlooked, partly because it appears as a very limited set of solutions within a very small interval of the heating parameter. By comparison, Lucarini and Bodai applied a multistable system with coexisting attractors in order to reveal the bistability of the climate system (e.g., Garashchuk et al. 2019; Lucarini and Bodai 2019).

[4] Coexisting solutions at two time scales are not necessarily the same as coexisting chaotic and nonchaotic attractors. For example, coexisting slow and fast manifolds in Lorenz (1986) are nonchaotic. Coexisting slow and fast variables within coupled systems (e.g., Peña and Kalnay 2004; Mitchell and Gottwald 2012) are chaotic. Lorenz (1990) applied his 1984 model (Lorenz 1984) for illustrating the coexistence of two oscillatory solutions.

GLM using three, five, seven, and nine modes revealed a continuously improved representation of temperature associated with additional smaller-scale modes.

Mathematically, our selection of new Fourier modes extends the nonlinear feedback loop and introduces new nonlinear coupling terms and new ODEs. As a result of nonlinear coupling terms that couple existing and new ODEs, a hierarchical scale dependence can be found within a high-dimensional LM (Shen 2016). Additionally, negative feedback by small-scale processes can be aggregated in order to provide a stronger effective dissipation for stabilizing solutions in higher dimensional Lorenz models. Thus, the GLM with a larger number of modes requires a larger heating parameter for the onset of chaos (Shen 2019a; Shen et al. 2019), yielding better predictability.[5] Other than the above, the aggregated negative feedback enables the appearance of stable equilibrium points within the GLM with nine or more modes, leading to two kinds of attractor coexistence.

[5] This is a unique feature of the GLM. In general, within a nonlinear PDE system, simply adding more Fourier modes does not necessarily produce a higher-dimensional system of ODEs that improves predictability as compared to a lower-dimensional system. As discussed on pages 8–10 of the supplemental materials for Shen (2016; https://npg.copernicus.org/preprints/2/C466/2015/npgd-2-C466-2015.pdf), our GLM can use fewer Fourier modes in order to produce a model with better predictability, as compared to other Lorenz-type models.

For example, as discussed in Shen (2019a), the first kind of attractor coexistence that consists of steady-state and chaotic solutions appears at a "moderate" heating parameter (e.g., $r = 680$). At a large heating parameter (e.g., $r = 1{,}600$), Shen (2019a) illustrated the second kind of attractor coexistence that contains steady-state and limit cycle solutions. *As shown in Fig. 2, ensemble runs with 128 members reveal how chaotic and nonchaotic solutions with distinct intrinsic predictability appear within different portions of the X–Y phase space (see details in Shen et al. 2019).* Within chaotic solutions, the degree of finite predictability varies, as suggested in Fig. 1 of Slingo and Palmer (2011). Other than the above, the coexistence of two periodic solutions with different periods has also been documented (e.g., Fig. 8 of Shen 2019a).

A REVISED VIEW WITH THE ALTERNATIVE AND CONCURRENT APPEARANCE OF VARIOUS TYPES OF SOLUTIONS. To better reveal the complexities of weather and climate, we discuss the alternative and concurrent appearance of various types of solutions associated with the time-varying heating function in Table 2, yielding $r \in [680, 1{,}720]$. Figures 3a and 3b display three trajectories and the heating function for $\tau \in [0, 5\pi T]$. Figures 3c–e *sequentially reveal three chaotic orbits, the first kind of attractor coexistence, and the second kind of attractor coexistence, respectively.* The results are consistent with those in Shen (2019a) that kept the heating parameter as a constant during numerical integration. Figure 3f displays the "coherent" variation of the nearly steady-state solution and the heating function for $\tau \in [30, 78]$.

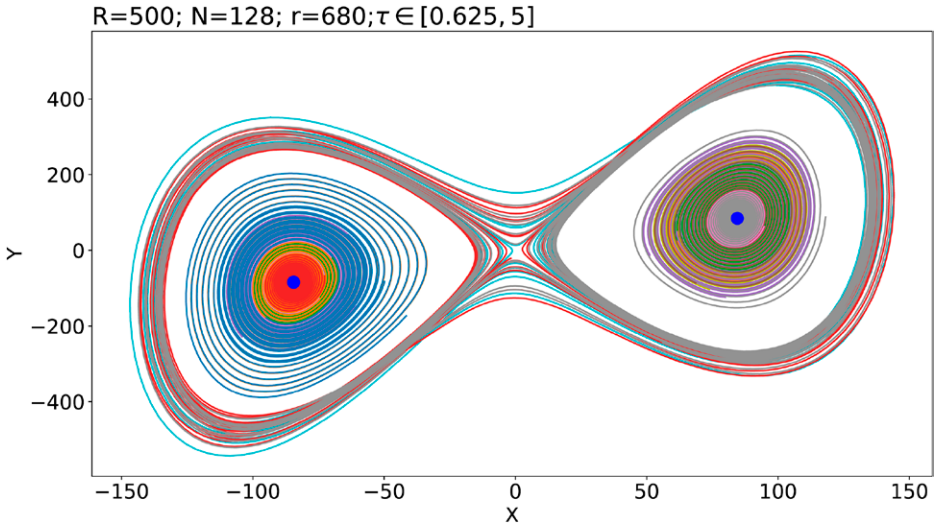

Fig. 2. The first kind of attractor coexistence within the generalized Lorenz model. There are 128 orbits in different colors, beginning with different initial conditions (ICs) for $\tau \in [0.625, 5]$ with $r = 680$. Chaotic orbits recurrently return close to the saddle point at the origin. Nonchaotic orbits eventually approach one of two stable critical points, as shown with large blue dots. Chaotic and nonchaotic orbits occupy different regions of attraction within the phase space.

Additional new insights from Fig. 3 include the following: 1) The first appearance of attractor coexistence with two different attractors, originally from nearby trajectories, indicates the so-called *final state sensitivity* (Grebogi et al. 1983) (i.e., whether or not the "final state" is a chaotic or steady state solution depends on initial conditions). 2) Although the two trajectories become chaotic with SDIC after $\tau > 21.25$, they become oscillatory solutions with very comparable amplitudes and frequencies after a long time integration, $\tau \in [40, 42]$. As a result, SDIC is not well defined during the epoch of the second kind of attractor coexistence since, in particular, ICs for weather can be continuously obtained. 3) Figure 3f indicates that once a "steady state" solution appears (when it reaches an equilibrium state with zero local time changes for all state variables), it remains "steady" and varies with the time-dependent heating function.[6] Such a feature cannot be found within the 3DLM because its nontrivial equilibrium points are not stable for $r > 24.74$. As a result, the appearance of stable equilibrium within the GLM effectively inhibits chaotic growth for some initial tiny perturbation, indicating the role of aggregated negative feedback. 4) Three major time scales for oscillatory or chaotic components can be identified: a large temporal scale (i.e., at the time scale of the

[6] Within both the 3DLM and GLM, as well as in other autonomous dissipative systems, the existence of a nontrivial equilibrium point suggests that corresponding steady-state solutions remain at a nonzero constant (i.e., they will not completely dissipate). On the other hand, since the stable steady-state solution of the 9DLM remains nearly "stationary" when heating parameters smoothly increase, such a stable solution may effectively dissipate as a result of the inclusion of other dissipative processes.

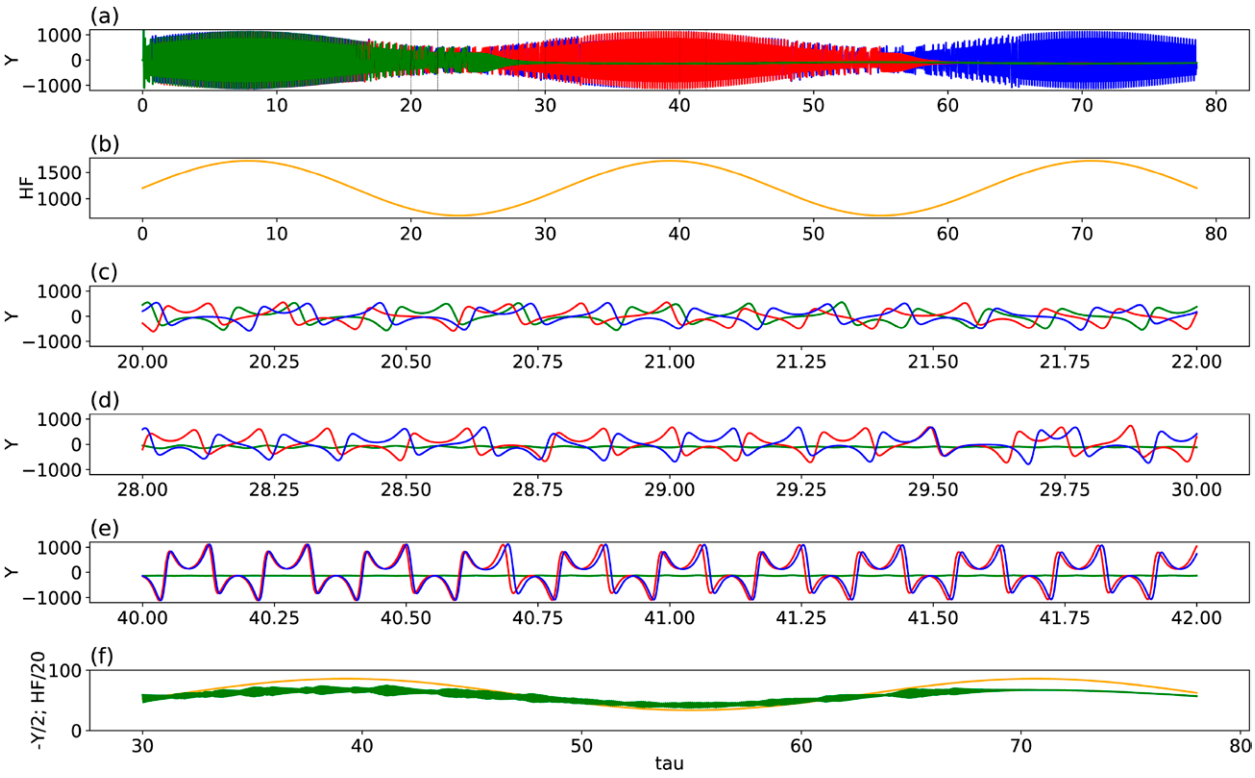

Fig. 3. The alternative and concurrent appearance of various types of solutions modulated by the periodic heating function, $r = r_0 + r_1 \sin(\tau/T)$, within the GLM. The color scheme and layout are as in Fig. 1. (a),(b) The three orbits of the control and parallel runs and the heating function. For parallel runs, the initial tiny perturbations are $\varepsilon = 10^{-8}$ and $\varepsilon = -10^{-8}$, respectively. (c) $\tau \in [20, 22]$ reveals chaotic solutions. (d) The first kind of attractor coexistence, consisting of chaotic solutions and a steady-state solution, is shown for $\tau \in [28, 30]$. (e) $\tau \in [40, 42]$ displays the second kind of attractor coexistence, including nonlinear oscillatory solutions and steady-state solutions. Interestingly, two orbits that appear chaotic at earlier times become regularly oscillatory with comparable amplitudes and phases. (f) A nearly steady-state solution ($-Y/2$) and the heating function $r(\tau)/20$ for $\tau \in [30, 78]$, showing a unique feature of the GLM as compared to the 3DLM.

heating function) in the slowly varying, stable steady-state solutions (e.g., Fig. 3f), as well as the "envelope" of entire solutions (e.g., Fig. 3a), medium temporal scales for nonlinear oscillatory solutions (e.g., Fig. 3e), and small temporal scales within transient oscillatory components of steady-state solutions and chaotic solutions. 5) *The alternative and concurrent appearance of various types of solutions indicate the complexities of weather and climate that possess both chaotic and regular processes*.

Conclusions and outlook

In this study, in contrast to the conventional view of "weather is chaotic," we suggest a refined view that the entirety of weather possesses both chaos and order. Such a revised view is fundamentally different from the Laplacian view of deterministic predictability and the Lorenz view of deterministic chaos. The refined view that turns our attention to coexisting multiple attractors from single attractors suggests both potential and challenges for improving our understanding of predictability and prediction for weather, as well as climate, as summarized below.

Within the GLM, two major physical processes that determine the alternative and/or concurrent appearance of various types of solutions and their distinct predictability are

1) the aggregated negative feedback of small-scale processes, indicating the potential role of improved accuracy (via an increase of vertical resolution or improved physical processes) in stabilizing the system;
2) modulation through a slowly varying heating function that may represent either temporal or spatial variations of "forcing" (e.g., radiation), yielding different predictability over different time periods or regions.

From a modeling perspective, this slowly varying forcing may be analogous to internal forcings such as large-scale waves that provide the determinism of tropical cyclone activities or external forcings such as slow processes that come from ocean or land model components.

In addition to determinism by large-scale forcing, predictability among various types of solutions displays a dependence on 1) initial conditions (e.g., via SDIC or the final state sensitivity), 2) model parameters (e.g., leading to chaotic and/or nonchaotic solutions), and 3) number of modes (e.g., yielding single attractors or multiple coexisting attractors). Chaotic processes display a sensitivity to initial conditions and possess finite intrinsic predictability. However, finite (practical) predictability within a real-world model may appear as a result of different mechanisms, including linear instability and/or computational chaos (Lorenz 1989; also see Table 1). For nonchaotic, steady-state or nonlinear oscillatory solutions, their intrinsic predictability is deterministic (e.g., up to the lifetime of a dissipative solution or the time interval of the epoch for oscillatory solutions) and, thus, their practical predictability may be continuously increased by improving the accuracy of the model and the initial conditions.

A limit of (practical) predictability of 2 weeks that has been proposed for decades was recently suggested for weather systems in the midlatitudes (Zhang et al. 2019). By comparison, our results suggest that better predictability for regular systems may locally appear in space and time (e.g., at extended-time or subseasonal to seasonal time scales) (e.g., Shen 2019b; Judt 2020), as illustrated below:

- A 10-yr, multiscale analysis of hurricanes and African easterly waves (AEWs; Wu and Shen 2016) indicated a near-constant annual number of AEWs, with the number shifting between 26 and 30 for 9 of the 10 study years during the July–September period. Such a feature seems to suggest "stable" large-scale forcing that may appear as a result of heating

over the African continent that contributes to a strong baroclinic zone along the boundary in the Sahel of central and eastern Africa.

- Based on the dynamics of limit cycle solutions, Shen (2019b) hypothesized that a balance between strong heating and nonlinearity[7] may lead to the "recurrence" of multiple AEWs.
- Although it may be challenging to predict the onset of an epoch for nonlinear oscillatory solutions, as shown in Fig. 3, better predictability is expected within such an epoch. The lead author and his coauthors (e.g., Shen et al. 2010; Shen 2019b) presented realistic 30-day simulations for the recurrence of multiple AEWs and the formation, movement, and intensification of Hurricane Helene (2006) between day 22 and 30. Such results were verified in a modeling sensitivity study with changes in dynamics and physical initial conditions.

To understand, verify, and improve the model's performance in predictions, additional suggestions and/or important concepts are provided below:

- Since SDIC does not always appear, initial tiny perturbations do not always contaminate numerical simulations.
- The presence of oscillatory (or saturated) root-mean-square average forecast errors for ensemble runs can help check whether oscillatory (or chaotic) solutions dominate over the target regions or periods (Liu et al. 2009). A focus on oscillatory types of solutions using models and observations may be effective for understanding intrinsic predictability at extended-range time scales and subseasonal to seasonal scales. However, depending on the periods of oscillatory systems, oscillatory features may not be detectable in short-term (~5–7-day) predictions or may appear in the form of computational chaos. An improved error growth model that can reveal saturated or oscillatory errors is required.
- As a result of final state sensitivity, it is important, but challenging, to detect the boundary between the basins of attraction for different attractors, in particular for a given initial condition that is close to a fractal boundary of a so-called riddled basin (e.g., Alexander et al. 1992; Cazelles 2001; also see Table 1). A systematic analysis of "outliers" among different ensemble runs may provide insights on the existence of multiple stability.
- Additionally, by taking intransitivity into consideration (Lorenz 1990; Pielke and Zeng 1994; also see Table 1), a different level of challenge in long-term prediction appears when transitivity occurs.
- In contrast to regular forcing, large-scale irregular forcing [e.g., El Niño that was shown to be "chaotic" by Guckenheimer et al. (2017)] could also modulate small-scale processes, increasing uncertainties in predictions. By comparison, small-scale processes may introduce additional heating in order to destabilize the system (e.g., Shen 2015, 2017). As such, identifying forcing terms and understanding their trends (e.g., growing or decaying) are important for better understanding their collective impact with nonlinearity on model simulations.
- To verify the refined view (that contains attractor coexistence, SDIC, final state sensitivity, and intransitivity) using numerical weather prediction models or observations, new analysis methods [e.g., for classifying basins of attraction (Sprott and Xiong 2015) and for revealing and detecting recurrence (Reyes and Shen 2019)] are required.

[7] Pedlosky and Frenzen (1980) discussed chaotic and nonchaotic solutions using a quasigeostrophic model that is mathematically identical to the 3DLM and suggested that the features of the 3DLM are directly applicable to the model of a weakly nonlinear baroclinic wave (also see Pedlosky 2019). Limit cycle solutions have been applied for studying the dynamics of quasi-biennial oscillation (e.g., Renaud et al. 2019) and vortex shedding (e.g., Noack and Eckelmann 1994; Ramesh et al. 2015). In comparison, by revealing multiple, stable, steady-state solutions in a low-order (six-dimensional) model based on a quasi-geostrophic system, Charney and DeVore (1979) suggested that atmospheric blocking, with resultant longer predictability, may appear in the form of a stable steady-state solution, due to a balance of nonlinearity, thermal forcing, Ekman damping, and topography (e.g., Crommelin et al. 2004; Chen and Xiong 2016). Such a feature indicates the importance of (mechanic) topographic forcing. This study focuses on the collective impact of nonlinearity and time-varying heating, as well as dissipation on oscillatory features.

- To overcome barriers that are holding back further advancement in predictability research, it is important to assess the ability of model ensemble predictions in bracketing and differentiating types of uncertainties in the context of intrinsic predictability that is only dependent on the flow itself, and practical predictability that is limited by imperfect initial conditions and/or (mathematical) formulas.

Acknowledgments. We thank reviewers of the manuscript, the editor (Dr. M. Alexander), and Drs. M. Ghil, F. Judt, J. Pedlosky, and Ms. T. Reyes for valuable comments, discussions, and help. The lead author is grateful for support from the Division of Graduate Affairs at San Diego State University.

For further reading

Alexander, J. C., J. Yorke, Z. You, and I. Kan, 1992: Riddled basin. *Int. J. Bifurcation Chaos*, **02**, 795–813, https://doi.org/10.1142/S0218127492000446.

Cazelles, B., 2001: Dynamics with riddled basins of attraction in models of interacting populations. *Chaos Solitons Fractals*, **12**, 301–311, https://doi.org/10.1016/S0960-0779(00)00047-3.

Charney, J. G., and J. G. DeVore, 1979: Multiple flow equilibria in the atmosphere and blocking. *J. Atmos. Sci.*, **36**, 1205–1216, https://doi.org/10.1175/1520-0469(1979)036<1205:MFEITA>2.0.CO;2.

Chen, Z.-M., and X. Xiong, 2016: Equilibrium states of the Charney-DeVore quasi-geostrophic equation in mid-latitude atmosphere. *J. Math. Anal. Appl.*, **444**, 1403–1416, https://doi.org/10.1016/j.jmaa.2016.07.021.

Crommelin, D. T., J. D. Opsteegh, and F. Verhulst, 2004: A mechanism for atmospheric regime behavior. *J. Atmos. Sci.*, **61**, 1406–1419, https://doi.org/10.1175/1520-0469(2004)061<1406:AMFARB>2.0.CO;2.

Faghih-Naini, S. and B.-W. Shen, 2018: Quasi-periodic orbits in the five-dimensional nondissipative Lorenz model: The role of the extended nonlinear feedback loop. *Int. J. Bifurcation Chaos*, **28**, 1850072, https://doi.org/10.1142/S0218127492000446.

Franz, M., and M. Zhang, 1995: Suppression and creation of chaos in a periodically forced Lorenz system. *Phys. Rev. E*, **52**, 3558–3565, https://doi.org/10.1103/PhysRevE.52.3558.

Garashchuk, I. R., D. I. Sinelshchikov, A. O. Kazakov, and N. A. Kudryashov, 2019: Hyperchaos and multistability in the model of two interacting microbubble contrast agents. *Chaos*, **29**, 063131, https://doi.org/10.1063/1.5098329.

Ghil, M., P. Read and L. Smith, 2010: Geophysical flows as dynamical systems: The influence of Hide's experiments. *Astron. Geophys.*, **51**, 4.28–4.35, https://doi.org/10.1111/j.1468-4004.2010.51428.x.

Grebogi, C., S. W. McDonald, E. Ott, and J. A. Yorke, 1983: Final state sensitivity: An obstruction to predictability. *Phys. Lett. A*, **99**, 415–418, https://doi.org/10.1016/0375-9601(83)90945-3.

Guckenheimer, J., A. Timmermann, H. Dijkstra, and A. Roberts, 2017: (Un)predictability of strong El Niño events. *Dyn. Stat. Climate Syst.*, **2**, dzx004, https://doi.org/10.1093/CLIMSYS/DZX004.

Hilborn, R. C., 2000: *Chaos and Nonlinear Dynamics. An Introduction for Scientists and Engineers*. 2nd ed. Oxford University Press, 650 pp.

Jordan, D. W., and P. Smith, 2007: *Nonlinear Ordinary Differential Equations. An Introduction for Scientists and Engineers*. 4th ed. Oxford University Press, 560 pp.

Judt, F., 2020: Atmospheric predictability of the tropics, middle latitudes, and polar regions explored through global storm-resolving simulations. *J. Atmos. Sci.*, **77**, 257–276, https://doi.org/10.1175/JAS-D-19-0116.1.

Liu, H.-L., F. Sassi, and R. R. Garcia, 2009: Error growth in a whole atmosphere climate model. *J. Atmos. Sci.*, **66**, 173–186, https://doi.org/10.1175/2008JAS2825.1.

Lorenz, E., 1963a: Deterministic nonperiodic flow. *J. Atmos. Sci.*, **20**, 130–141, https://doi.org/10.1175/1520-0469(1963)020<0130:DNF>2.0.CO;2.

——, 1963b: The predictability of hydrodynamic flow. *Trans. New York Acad. Sci. Ser. II*, **25**, 409–432, https://doi.org/10.1111/J.2164-0947.1963.TB01464.X.

——, 1963c: The mechanics of vacillation. *J. Atmos. Sci.*, **20**, 448–464, https://doi.org/10.1175/1520-0469(1963)020<0448:TMOV>2.0.CO;2.

——, 1969: The predictability of a flow which possesses many scales of motion. *Tellus*, **21**, 289–307, https://doi.org/10.3402/tellusa.v21i3.10086.

——, 1972: Predictability: Does the flap of a butterfly's wings in Brazil set off a tornado in Texas? *Proc. 139th Meeting of AAAS Section on Environmental Sciences*, Cambridge, MA, AAAS, 5 pp., https://eaps4.mit.edu/research/Lorenz/Butterfly_1972.pdf.

——, 1984: Irregularity: A fundamental property of the atmosphere. *Tellus*, **36A**, 98–110, https://doi.org/10.1111/j.1600-0870.1984.TB00230.X.

——, 1986: On the existence of a slow manifold. *J. Atmos. Sci.*, **43**, 1547–1558, https://doi.org/10.1175/1520-0469(1986)043<1547:OTEOAS>2.0.CO;2.

——, 1989: Computational chaos: A prelude to computational instability. *Physica D*, **35D**, 299–317, https://doi.org/10.1016/0167-2789(89)90072-9.

——, 1990: Can chaos and intransitivity lead to interannual variability? *Tellus*, **42A**, 378–389, https://doi.org/10.3402/tellusa.v42i3.11884.

——, 1993: *The Essence of Chaos*. University of Washington Press, 227 pp.

——, 2006: Computational periodicity as observed in a simple system. *Tellus*, **58A**, 549–557, https://doi.org/10.1111/j.1600-0870.2006.00201.x.

Lucarini, V., 2019: Stochastic resonance for nonequilibrium systems. *Phys. Rev. E*, **100**, 062124, https://doi.org/10.1103/PhysRevE.100.062124.

——, and T. Bódai, 2019: Transitions across melancholia states in a climate model: Reconciling the deterministic and stochastic points of view. *Phys. Rev. Lett.*, **122**, 158701, https://doi.org/10.1103/PhysRevLett.122.158701.

Mitchell, L., and G. A. Gottwald, 2012: Data assimilation in slow–fast systems using homogenized climate models. *J. Atmos. Sci.*, **69**, 1359–1377, https://doi.org/10.1175/JAS-D-11-0145.1.

Moon, S., B.-S. Han, J. Park, J. M. Seo, and J.-J. Baik, 2017: Periodicity and chaos of high-order Lorenz systems. *Int. J. Bifurcation Chaos*, **27**, 1750176, https://doi.org/10.1142/S0218127417501760.

——, J. M. Seo, B.-S. Han, J. Park, and J.-J. Baik, 2019: A physically extended Lorenz system. *Chaos*, **29**, 063129, https://doi.org/10.1063/1.5095466.

——, ——, and J.-J. Baik, 2020: High-dimensional generalizations of the Lorenz system and implications for predictability. *Phys. Scr.*, **95**, 085209, https://doi.org/10.1088/1402-4896/ab9d3e.

Nese, J. M., 1989: Quantifying local predictability in phase space. *Physica D*, **35**, 237–250, https://doi.org/10.1016/0167-2789(89)90105-X.

Noack, B., and H. Eckelmann, 1994: A global stability analysis of the steady and periodic cylinder wake. *J. Fluid Mech.*, **270**, 297–330, https://doi.org/10.1017/S0022112094004283.

Park, J., B.-S. Han, H. Lee, Y.-L. Jeon, and J.-J. Baik, 2016: Stability and periodicity of high-order Lorenz–Stenflo equations. *Phys. Scr.*, **91**, 065202, https://doi.org/10.1088/0031-8949/91/6/065202.

Pedlosky, J., 1972: Limit cycles and unstable baroclinic waves. *J. Atmos. Sci.*, **29**, 53–63, https://doi.org/10.1175/1520-0469(1972)029<0053:LCAUBW>2.0.CO;2.

——, 2019: The effect of beta on the downstream development of unstable, chaotic baroclinic waves. *J. Phys. Oceanogr.*, **49**, 2337–2343, https://doi.org/10.1175/JPO-D-19-0097.1.

——, and C. Frenzen, 1980: Chaotic and periodic behavior of finite-amplitude baroclinic waves. *J. Atmos. Sci.*, **37**, 1177–1196, https://doi.org/10.1175/1520-0469(1980)037<1177:CAPBOF>2.0.CO;2.

Peña, M., and E. Kalnay, 2004: Separating fast and slow modes in coupled chaotic systems. *Nonlinear Processes Geophys.*, **11**, 319–327, https://doi.org/10.5194/npg-11-319-2004.

Pielke, R. A., and X. Zeng, 1994: Long-term variability of climate. *J. Atmos. Sci.*, **51**, 155–159, https://doi.org/10.1175/1520-0469(1994)051<0155:LTVOC>2.0.CO;2.

Ramesh, K., J. Murua, and A. Gopalarathnam, 2015: Limit-cycle oscillations in unsteady flows dominated by intermittent leading-edge vortex shedding. *J. Fluids Struct.*, **55**, 84–105, https://doi.org/10.1016/j.jfluidstructs.2015.02.005.

Renaud, A., L.-P. Nadeau, and A. Venaille, 2019: Periodicity disruption of a model quasibiennial oscillation of equatorial winds. *Phys. Rev. Lett.*, **122**, 214504, https://doi.org/10.1103/PhysRevLett.122.214504.

Reyes, T., and B.-W. Shen, 2019: A recurrence analysis of chaotic and non-chaotic solutions within a generalized nine-dimensional Lorenz model. *Chaos Solitons Fractals*, **125**, 1–12, https://doi.org/10.1016/j.chaos.2019.05.003.

Saltzman, B., 1962: Finite amplitude free convection as an initial value problem. *J. Atmos. Sci.*, **19**, 329–341, https://doi.org/10.1175/1520-0469(1962)019<0329:FAFCAA>2.0.CO;2.

Shen, B.-W., 2014: Nonlinear feedback in a five-dimensional Lorenz model. *J. Atmos. Sci.*, **71**, 1701–1723, https://doi.org/10.1175/JAS-D-13-0223.1.

——, 2015: Nonlinear feedback in a six-dimensional Lorenz model: Impact of an additional heating term. *Nonlinear Processes Geophys.*, **22**, 749–764, https://doi.org/10.5194/npg-22-749-2015.

——, 2016: Hierarchical scale dependence associated with the extension of the nonlinear feedback loop in a seven-dimensional Lorenz model. *Nonlinear Processes Geophys.*, **23**, 189–203, https://doi.org/10.5194/NPG-23-189-2016.

——, 2017: On an extension of the nonlinear feedback loop in a nine-dimensional Lorenz model. Chaotic Model. Simul., 2, 147–157.

——, 2018: On periodic solutions in the non-dissipative Lorenz model: The role of the nonlinear feedback loop. *Tellus*, **70A**, 1471912, https://doi.org/10.1080/16000870.2018.1471912.

——, 2019a: Aggregated negative feedback in a generalized Lorenz model. *Int. J. Bifurcation Chaos*, **29**, 1950037, https://doi.org/10.1142/S0218127419500378.

——, 2019b: On the predictability of 30-day global mesoscale simulations of African easterly waves during summer 2006: A view with the generalized Lorenz model. *Geosciences*, **9**, 281, https://doi.org/10.3390/GEOSCIENCES9070281.

——, 2020: Homoclinic orbits and solitary waves within the non-dissipative Lorenz model and KdV equation. *Int. J. Bifurcation Chaos*, **30**, 2050257, 1–15, https://doi.org/10.1142/S0218127420502570.

——, 2021: Solitary waves, homoclinic orbits, and nonlinear oscillations within the non-dissipative Lorenz model, the inviscid Pedlosky model, and the KdV equation. *Proc. 13th Chaos Int. Conf., CHAOS 2020*, C. H. Skiadas and Yiannis Dimotikalis, Eds., *Springer Proceedings in Complexity*, Springer, https://doi.org/10.13140/RG.2.2.26813.90089, in press.

——, W.-K. Tao, and M.-L. C. Wu, 2010: African easterly waves in 30-day high-resolution global simulations: A case study during the 2006 NAMMA period. *Geophys. Res. Lett.*, **37**, L18803, https://doi.org/10.1029/2010GL044355.

——, T. A. L. Reyes, and S. Faghih-Naini, 2019: Coexistence of chaotic and non-chaotic orbits in a new nine-dimensional Lorenz model. *11th Chaotic Modeling and Simulation Int. Conf.*, Rome, Italy, CMSIM, 239–255, https://doi.org/10.1007/978-3-030-15297-0_22.

——, R. A. Pielke Sr., X. Zeng, J.-J. Baik, S. Faghih-Naini, J. Cui, R. Atlas, and T. A. Reyes, 2021: Is weather chaotic? Coexisting chaotic and non-chaotic attractors within Lorenz models. *Proc. 13th Chaos Int. Conf., CHAOS 2020*, C. H. Skiadas and Yiannis Dimotikalis, Eds., *Springer Proceedings in Complexity*, Springer, in press.

Shimizu, T., 1979: Analytic form of the simplest limit cycle in the Lorenz model. *Physica A*, **97A**, 383–398, https://doi.org/10.1016/0378-4371(79)90113-4.

Slingo, J., and T. Palmer, 2011: Uncertainty in weather and climate prediction. *Philos. Trans. Roy. Soc*, **369A**, 4751–4767, https://doi.org/10.1098/RSTA.2011.0161.

Smith, R. K., and J. M. Reilly, 1977: On a theory of amplitude vacillation in baroclinic waves: Some numerical solutions. *J. Atmos. Sci.*, **34**, 1256–1260, https://doi.org/10.1175/1520-0469(1977)034<1256:OATOAV>2.0.CO;2.

Sparrow, C., 1982: *The Lorenz Equations: Bifurcations, Chaos, and Strange Attractors*. Springer, 269 pp.

Sprott, J. C., and A. Xiong, 2015: Classifying and quantifying basins of attraction. *Chaos*, **25**, 083101, https://doi.org/10.1063/1.4927643.

——, J. A. Vano, J. C. Wildenberg, M. B. Anderson, and J. K. Noel, 2005: Coexistence and chaos in complex ecologies. *Phys. Lett. A*, **335**, 207–212, https://doi.org/10.1016/J.PHYSLETA.2004.12.068.

——, X. Wang, and G. Chen, 2013: Coexistence of point, periodic and strange attractors. *Int. J. Bifurcation Chaos*, **23**, 1350093, https://doi.org/10.1142/S0218127413500934.

Thompson, J. M. T., and H. B. Stewart, 2002: *Nonlinear Dynamics and Chaos*. 2nd ed. John Wiley and Sons, 437 pp.

Wu, Y.-L., and B.-W. Shen, 2016: An evaluation of the parallel ensemble empirical mode decomposition method in revealing the role of downscaling processes associated with African easterly waves in tropical cyclone genesis. *J. Atmos. Oceanic Technol.*, **33**, 1611–1628, https://doi.org/10.1175/JTECH-D-15-0257.1.

Yorke, J., and E. Yorke, 1979: Metastable chaos: The transition to sustained chaotic behavior in the Lorenz model. *J. Stat. Phys.*, **21**, 263–277, https://doi.org/10.1007/BF01011469.

Zeng, X., R. A. Pielke Sr., and R. Eykholt, 1993: Chaos theory and its applications to the atmosphere. *Bull. Amer. Meteor. Soc.*, **74**, 631–644, https://doi.org/10.1175/1520-0477(1993)074<0631:CTAIAT>2.0.CO;2.

Zhang, F., Y. Q. Sun, L. Magnusson, R. Buizza, S.-J. Lin, J.-H. Chen, and K. Emanuel, 2019: What is the predictability limit of midlatitude weather? *J. Atmos. Sci.*, **76**, 1077–1091, https://doi.org/10.1175/JAS-D-18-0269.1.